Multirate repetitive control for an industrial print-belt system

Aarnoudse, Leontine; Cox, Kevin; Koekebakker, Sjirk; Oomen, Tom

Citation (APA)
Aarnoudse, L., Cox, K., Koekebakker, S., & Oomen, T. (2024). Multirate repetitive control for an industrial print-belt system. *Mechatronics*, *100*, Article 103187. https://doi.org/10.1016/j.mechatronics.2024.103187

Important note
To cite this publication, please use the final published version (if applicable).
Please check the document version above.

Multirate repetitive control for an industrial print-belt system[☆],[☆☆]

Leontine Aarnoudse [a],[*], Kevin Cox [a], Sjirk Koekebakker [a],[b], Tom Oomen [a],[c]

[a] *Department of Mechanical Engineering, Control Systems Technology, Eindhoven University of Technology, Eindhoven, The Netherlands*
[b] *Canon Production Printing, The Netherlands*
[c] *Delft Center for Systems and Control, Delft University of Technology, Delft, The Netherlands*

ARTICLE INFO

ABSTRACT

The increasing complexity of next-generation mechatronic systems leads to different types of periodic disturbances, which require dedicated repetitive control strategies to attenuate. The aim of this paper is to develop a new repetitive control strategy to completely attenuate a periodic disturbance and a user-defined number of relevant higher harmonics with limited memory usage. To this end, a multirate repetitive controller is developed, which combines a buffer at a reduced sampling rate with learning and robustness filters at the original sampling rate of the system. This leads to a linear periodic time-varying system, for which convergence conditions are developed. The method is implemented on an industrial print-belt system, demonstrating that it can match the performance of traditional repetitive control while significantly reducing the memory usage.

1. Introduction

Next-generation mechatronic systems need to meet ever-increasing requirements in terms of speed and accuracy, leading to increasingly complicated designs with many moving components. These components often introduce periodic disturbances with different characteristics. For example, an industrial print belt consists of different rollers and drive belts, as well as a long, flexible print belt, all of which introduce periodic disturbances at varying frequencies, and with a varying number of higher harmonics that contribute to the total error. Repetitive control (RC) is capable of attenuating periodic disturbances completely, leading to high performance for mechatronic systems. The main idea of RC is to use a periodic signal generator to fully reject periodic signals [1,2], in accordance with the internal model principle [3]. The different types of periodic disturbances occurring in next-generation systems each require different repetitive control strategies to be attenuated.

Traditional repetitive control compensates the periodic disturbance and its higher harmonics up to the Nyquist frequency, which is a suitable approach for disturbances with a large number of relevant higher harmonics, but which has disadvantages for other types of disturbances. The repetitive controller introduces local disturbance suppression at the base frequency and its multiples, and consequently disturbances at other frequencies are amplified due to the waterbed effect [2]. In addition, when high sampling frequencies are combined with low

disturbance frequencies, traditional RC requires a large buffer. This may lead to memory shortages when multiple repetitive controllers are needed to compensate multiple disturbances with different base frequencies.

In practice, for many disturbances only a small number of higher harmonics contribute significantly to the error, and it is often not necessary to compensate all disturbance harmonics up to the Nyquist frequency. Different approaches have been developed to increase the flexibility regarding the number of higher harmonics that is attenuated, including using the low-pass robustness filter that is necessitated by modeling inaccuracies in traditional RC [2], and low-order [4] and low-rate RC [5] approaches. The low-pass filter in traditional RC provides robustness, but it also reduces the effectiveness of the repetitive controller at high frequencies, thus rendering the high-frequency content of the buffer redundant. This is an inefficient way to also limit the number of harmonics that is suppressed, because it leads to non-intuitive design, the RC buffer remains unnecessarily large, and it may increase the steady-state error [4].

Low-order repetitive control [4] models only some of the harmonics, using individual functions to model each of the frequencies. Similar ideas are developed in [6–8], where the buffer-based periodic signal generator is replaced by a small number of sine or cosine functions. This matched basis functions repetitive controller generates a disturbance-compensating signal at specific frequencies without any harmonics. This approach is especially suitable for disturbances which have no

relevant higher harmonics, or only a small number of them. When the number of relevant harmonics increases, more basis functions are needed which increases the computational cost significantly [6].

Low-rate repetitive control [5] enables attenuating a user-defined number of higher harmonics by designing the repetitive controller at a lower sampling rate than the original system. To this end, down- and upsampling are applied to the signals entering and exiting the repetitive controller. The low-rate implementation of the repetitive controller significantly reduces the memory usage, and similar to regular RC, stability can be guaranteed through design of robustness filters. This method has been applied successfully to, e.g., gantry-type robots [5] and PWM DC/AC converters [9].

Note that while the method in [5,9] is often called 'multirate', it is here referred to as 'low-rate' to indicate that the complete repetitive controller, including the buffer and the learning filter, is implemented at a lower sampling rate. This has two disadvantages. First, the low-rate learning filter is typically a worse approximation of the inverse closed-loop round the low-rate Nyquist frequency compared to a high-rate learning filter. Second, the low-rate implementation may lead to a mismatch between the disturbance frequency and the frequency generated by the repetitive controller, leading to reduced attenuation or even amplification of this disturbance. As a result, low-rate RC is often not able to match the performance of traditional repetitive control.

Several other multirate repetitive control methods exist that aim at solving different types of problems, yet none address the problem considered here. In [10,11], a multirate repetitive controller is developed with different input and output sampling rates, exploiting an actuator sampling rate which is much higher than the sensor sampling rate to attenuate intersample disturbances. In [12], sampled-data H_∞ delayed signal reconstruction is applied to this same multirate setting. In [13], control signals with fractional-order periods are generated by designing an internal model at a sampling frequency different from that of the system, similar to the approach in low-order RC. This is applied successfully to laser-based additive manufacturing. In [14], a repetitive controller is developed that is capable of adapting to varying disturbance frequencies in a fractional-order RC scheme.

Although significant steps have been taken to develop repetitive controllers to attenuate a user-defined number of harmonics of periodic disturbances, at present it is not clear how to achieve the performance of traditional RC with a low memory usage of the buffer. The aim of this paper is to develop a multirate repetitive controller in which only the buffer is implemented at a reduced sampling rate, while implementing learning filters and period-mismatch compensation at the original high sampling rate of the system. The contribution consists of the following elements.

- A multirate repetitive controller that implements only the buffer at a reduced sampling rate.
- Stability conditions for the linear periodic time-varying system that results from the multirate characteristics of the controller.
- Comparison to related low-rate and traditional RC methods, theoretically and through implementation on an industrial print-belt system.

This paper is structured as follows. In Section 2, traditional RC and the problem considered in this paper are introduced. In Section 3, the multirate repetitive controller is introduced. Stability conditions are developed in Section 4. In Section 5, the approach is compared to low-rate repetitive control. Experimental results are presented in Section 6, and finally conclusions are given in Section 7.

2. Problem formulation

In this section the problem considered in this paper is formulated. First, an industrial print-belt system is introduced as a motivating example. This system is also used in the experimental case study in Section 6. Second, repetitive control is introduced as a method to attenuate periodic disturbances in this system, and third, some limitations are identified which lead to the problem definition.
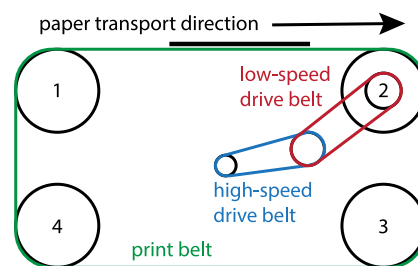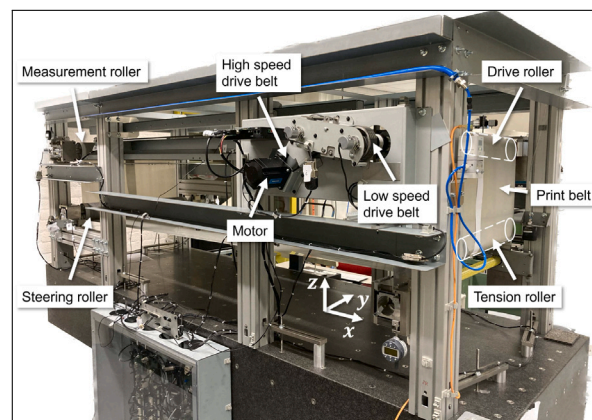

Fig. 1. Industrial print-belt system (top) and schematic representation (bottom). The aim is to transport paper on the print belt (——) with a constant velocity. The rollers (1: measurement roller, 2: drive roller, 3: tension roller, 4: steering roller) and drive belts (high-speed (——) and low-speed (——)) induce various repeating disturbances in the system.

2.1. Case study: industrial print-belt system

Consider the industrial print-belt system shown in Fig. 1. The system is identified in closed-loop using multisines, leading to the frequency response function of the complementary sensitivity shown in Fig. 2. The feedback controller consists of proportional action based on the output of the measurement roller and derivative action based on the motor position. Fig. 2 shows the transfer seen by a repetitive controller that is added to the feedback loop based on the measurement roller. The motor feedback loop is included using an equivalent plant approach.

A print belt handles media in the heart of the printer, by transporting paper sheets beneath the printing process that consists of inkjet printheads. This requires the system to transport paper with a constant velocity, during which the rollers and drive belts introduce repeating disturbances at various frequencies, which also have varying numbers of relevant higher harmonics. The fundamental frequencies of these disturbances are identified using demodulation, based on initial estimates that follow from the dimensions of the belt and rollers. The error spectrum of this system is shown in Fig. 3 and contains disturbances caused by the low-speed and high-speed drive belts, occurring at respectively 1.7 Hz and 5.4 Hz. These disturbances have a small number of approximately 15 and 7 relevant higher harmonics. In addition, there is a disturbance originating from the print belt at 0.23 Hz with significant higher harmonics up to an order of 50, and multiple disturbances around 3.7 Hz that are caused by the rollers, which have no significant higher harmonics. The system also contains non-periodic disturbances such as noise.

2.2. Repetitive control

Repetitive control is capable of attenuating periodic disturbances perfectly by including a buffer-based periodic signal generator in the feedback path according to the internal model principle [3]. Consider
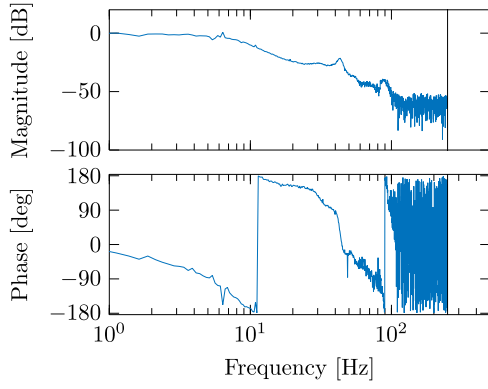
Fig. 2. Bode diagram of the measured frequency response of the closed loop $T = (1 + PC)^{-1}PC$ (——).
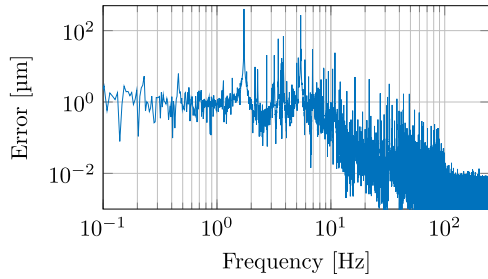

Fig. 3. Error spectrum of the print-belt system without repetitive control. The disturbances originating from the low-speed and high-speed drive belts are visible at respectively $1.7\,\text{Hz}$ and $5.4\,\text{Hz}$.
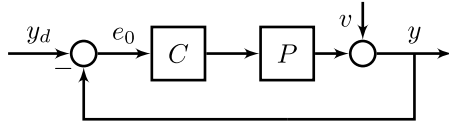

Fig. 4. Closed-loop control scheme with system P and controller C.

the industrial print belt system as a single-input, single-output (SISO), linear time-invariant (LTI) system P in feedback with a controller C as illustrated in Fig. 4. The error e_0 of this system is described by

$$e_0 = \underbrace{(1 + PC)^{-1}}_{S}(y_d - v),\tag{1}$$

for a reference y_d and a disturbance term v. The error signal has periodic and non-periodic components due to periodic and non-periodic disturbances. To compensate for a single periodic disturbance and its higher harmonics, a repetitive controller can be implemented as shown in Fig. 5. This leads to an error e given by

$$e = (1 + PC(1 + R))^{-1}(y_d - v) = \underbrace{(1 + TR)^{-1}}_{S_R} e_0,\tag{2}$$

where S_R denotes the modifying sensitivity and $T = PC(1+PC)^{-1}$, see, e.g., [15] for a derivation. The repetitive controller R is given by

$$R(z) = \frac{\alpha L(z)z^{-N}Q(z)}{1 - z^{-N}Q(z)},\tag{3}$$

where the delay operator z^{-N} acts as a buffer, storing the error signal of the previous repetition. The base buffer size $N \in \mathbb{N}$ is typically chosen such that it approximately contains an integer number of periods of the periodic disturbance. For example, if the high-rate sampling frequency of the system $f_h = 500\,\text{Hz}$, a disturbance frequency of $f_d = 5\,\text{Hz}$ would give $N = 100$. For $f_d = 8\,\text{Hz}$ a buffer of $N = 63$ includes approximately
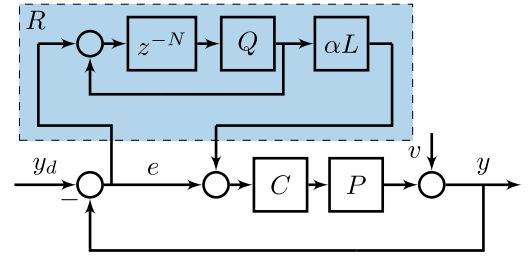

Fig. 5. Closed-loop control scheme with repetitive controller R.
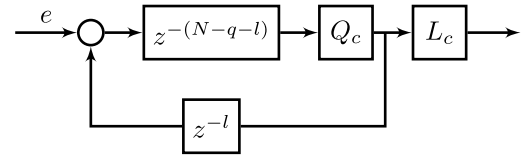

Fig. 6. Repetitive controller R. The preview for filters L and Q, consisting of respectively l and q samples, is embedded by taking the buffer as $z^{-(N-q-l)}$.

one period, alternatively a larger buffer of $N = 125$ could be used that includes exactly two periods. Here, the base buffer size N is taken as

$$N = \text{round}\left(\frac{f_h}{f_d}\right),\tag{4}$$

i.e., the integer buffer size is chosen that best approximates one period of the disturbance frequency f_d. The learning gain is denoted by $\alpha \in (0, 1]$, where a small value reduces the influence of non-periodic disturbances and ensures safe operation, at the cost of convergence speed. The robustness filter $Q(z) \in \mathcal{R}$ and learning filter $L(z) \in \mathcal{R}$ can be non-causal, in the sense that these filters can have finite preview of respectively q and l samples. In that case, the causal versions Q_c and L_c are implemented, and the finite preview is embedded in the buffer, replacing z^{-N} by z^{-N_s} with $N_s = N - l - q$ such that $R(z) \in \mathcal{RH}_\infty$ is real-rational, causal and stable. In addition, the preview of L is also included in the backward path of the repetitive controller. The embedding of this preview in the delay is illustrated in Fig. 6. Typically, L is chosen as an approximation of T^{-1}, for example using ZPETC [16], and Q is a finite impulse response (FIR) low-pass filter.

2.3. Problem formulation

The repetitive control approach described in the previous paragraph is suitable for compensating one periodic disturbance with many relevant higher harmonics, but for complicated mechatronic systems such as the industrial print-belt system in Fig. 1, it has significant limitations. The print-belt system is sampled at a sampling frequency f_h of 500 Hz, which is high compared to the base frequencies of the disturbances, which are between 0.2 and 6 Hz. This leads to an unnecessarily large buffer size N, which becomes problematic when the system contains multiple periodic disturbances that each require a dedicated repetitive controller to attenuate. In addition, standard repetitive controllers compensate a periodic disturbance and all its higher harmonics up to the Nyquist frequency, even in cases where only a limited number of higher harmonics contribute significantly to the error and can effectively be learned due to model quality issues. This unnecessary attenuation at high frequencies leads to amplification of frequencies around the higher harmonics due to the waterbed effect.

The industrial print-belt system contains three types of disturbances. The first is the disturbance introduced by the print belt at 0.23 Hz, which has significant higher harmonics up to an order of 50. For this disturbance, attenuating the higher harmonics up to the Nyquist frequency is useful and therefore, a standard repetitive controller is
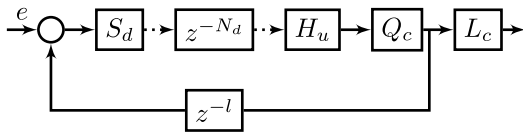
Fig. 7. Multirate repetitive controller with downsampler S_d and upsampler H_u. The preview required for Q and L is embedded in the low-rate buffer size $N_d = \text{round}(\frac{N-l-q}{F})$. Low-rate signals are indicated by dotted lines.

Fig. 8. Multirate repetitive controller with anti-aliasing filter B_a which introduces a delay a that is compensated for in the buffer, downsampler S_d and cubic-splines upsampler CS_u which requires a preview u. The preview required for B_a, L and the cubic-splines upsampling is embedded in the low-rate buffer size $N_s = N_{df} - u_d$. The additional delay term $z^{-\zeta}$ compensates for period discrepancies between the original buffer N and the low-rate buffer N_{df}. Low-rate signals are indicated by dotted lines.

suitable to attenuate this disturbance. The second type are the disturbances caused by the four rollers of the system, which occur around 3.7 Hz and which have no significant higher harmonics. Each of these disturbances can be attenuated perfectly by a periodic signal generator at a single frequency, i.e., a sinusoidal basis function as used in, e.g., [4,6–8].

The aim of this paper is to develop an accurate and efficient repetitive controller for the third type of disturbances in the print-belt system. The disturbances caused by the low- and high-speed drive belts occur at respectively 1.7 Hz and 5.4 Hz and have approximately 15 and 7 relevant higher harmonics. On the one hand, using a traditional repetitive controller to attenuate these disturbances leads to an unnecessarily large buffer and superfluous memory usage. On the other hand, attenuating all relevant higher harmonics with basis functions leads to a high computational load which is not feasible in a system that contains multiple disturbances. Attenuating these disturbances requires a repetitive controller that perfectly attenuates the periodic component of a disturbance at the fundamental frequency and a user-defined number of higher harmonics, while limiting the memory usage as well as amplification of non-periodic disturbances at high frequencies due to the waterbed effect.

3. Approach

In this section, a multirate repetitive controller is introduced that retains the performance of traditional repetitive control at a fraction of the memory usage. First, a basic multirate repetitive controller is introduced. Second, this multirate RC is extended with an anti-aliasing filter and cubic splines upsampling.

3.1. Multirate repetitive control

The main idea of multirate repetitive control is to implement the buffer, i.e, the delay operator z^{-N}, at a lower sampling rate, while all other components of the repetitive controller are implemented at the original sampling rate of the system. To this end, down- and upsamplers S_d and H_u are included before and after the buffer. This reduces the number of samples that is stored in the buffer and results in a multirate repetitive controller R_{MR} as illustrated in Fig. 7.

The buffer in this multirate repetitive controller has a low sampling rate f_l, which is related to the original sampling rate f_h through

$$f_l = \frac{f_h}{F} \tag{5}$$

for some user-defined downsampling factor $F \in \mathbb{N}$. The downsampled delay N_d is chosen as the integer delay that best approximates the downsampled disturbance frequency $\frac{f_d}{F}$ and is given by

$$N_d = \text{round}\left(\frac{N-l-q}{F}\right). \tag{6}$$

In practice, this multirate RC structure leads to decreased performance compared to traditional RC for multiple reasons. First of all, down- and upsampling of the error signal leads to aliasing and imaging, which should be compensated for. More importantly, the downsampling introduces discrepancies between the period of the disturbance and the period of the compensating signal generated by the repetitive
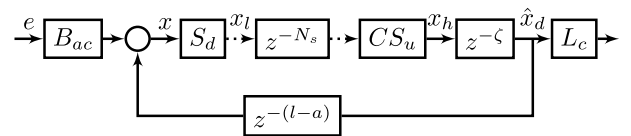
controller whenever $\frac{N}{N_d}$ is non-integer, which is often the case. Similarly, the downsampling of the embedded preview for Q and L leads to a mismatch. To counteract this period mismatch and reduce the effects of aliasing and imaging, three additional components are included in the multirate repetitive controller.

3.2. Multirate RC with cubic splines upsampling

To improve the performance of multirate RC, three components are included. This leads to the new multirate RC scheme illustrated in Fig. 8. First, to reduce the aliasing in the downsampling operation, an anti-aliasing filter B_a is included. This is an FIR low-pass filter which introduces a delay of a samples in the system. This delay is compensated for in the forward and backward part of the repetitive controller.

Secondly, the zero-order hold upsampler H_u is replaced by upsampling using cubic splines. Given a sample $x_l(k)$ of the low sampling rate signal x_l, and an integer ratio F between the high and low sampling rates according to (5), the high sampling rate reconstruction $x_h^k \in \mathbb{R}^F$ for the F high-rate samples between $x_l(k)$ and $x_l(k+1)$ is given by

$$
x_h^k = \begin{bmatrix} x_h((k-1)F+1) \\ x_h((k-1)F+2) \\ \vdots \\ x_h(kF) \end{bmatrix} = \tag{7}
$$

$$
\begin{bmatrix} 0 & 0 & 0 & 1 \\ \left(\frac{1}{F}\right)^3 & \left(\frac{1}{F}\right)^2 & \frac{1}{F} & 1 \\ \left(\frac{2}{F}\right)^3 & \left(\frac{2}{F}\right)^2 & \frac{2}{F} & 1 \\ \vdots & \vdots & \vdots & \vdots \\ \left(\frac{F-1}{F}\right)^3 & \left(\frac{F-1}{F}\right)^2 & \frac{F-1}{F} & 1 \end{bmatrix} \begin{bmatrix} 2 & -2 & 1 & 1 \\ -3 & 3 & -2 & -1 \\ 0 & 0 & 1 & 0 \\ 1 & 0 & 0 & 0 \end{bmatrix}
$$

$$
\cdot \begin{bmatrix} 0 & 1 & 0 & 0 \\ 0 & 0 & 1 & 0 \\ -\frac{1}{2} & 0 & \frac{1}{2} & 0 \\ 0 & -\frac{1}{2} & 0 & \frac{1}{2} \end{bmatrix} \begin{bmatrix} x_l(k-1) \\ x_l(k) \\ x_l(k+1) \\ x_l(k+2) \end{bmatrix}.
$$

Thus, a cubic spline is fitted through $x_l(k)$ and $x_l(k+1)$, and the derivatives at k and $k+1$ are approximated by the central difference, which also requires $x_l(k-1)$ and $x_l(k+2)$. The high-rate approximation x_h^k consists of F equidistantly spaced points on this spline. The cubic splines interpolation introduces a delay of $u_d = 2$ samples, which is compensated for in the buffer size N_s in the forward path of the repetitive controller. Note that this cubic splines interpolation consists of a matrix multiplication with relatively small matrices, which is computationally cheap.

The cubic splines act both as an upsampler and as a low-pass filter. Therefore, no additional Q-filter is needed in this approach. If the cubic splines are not sufficient to ensure stability at high frequencies, the learning filter L can be extended by a lowpass filter.

The third component that is included in the multirate repetitive controller is the high-sampling rate delay term $z^{-\zeta}$. This term compensates the period mismatch that results from the low-rate buffer, such that the

period mismatch does not exceed that of standard repetitive control. This is illustrated in the following example.

Example 1. Consider the printbelt system with a sampling rate of $f_s = 500$ Hz and a disturbance at 5.421 Hz. For a traditional repetitive controller, a suitable buffer size is given by $N = 92$, which approximates the period length of $\frac{500}{5.421} = 92.23$ with a small deviation of 0.25%. If a low-rate buffer with $f_l = 100$ Hz is used instead, the closest approximation of $\frac{100}{5.421} = 18.45$ is given by $N = 18$, which is upsampled with a factor $F = 5$ to 90 samples at the high rate, leading to a period mismatch of 2.5%. A compensation of $\zeta = 2$ samples at the high rate leads to a total high-rate period of the multirate repetitive controller of 92 samples, such that the period mismatch of the multirate RC does not exceed that of traditional RC.

The number of delays ζ is determined as follows. First, instead of rounding the low-rate buffer length to the nearest integer as in (6), the sum of all delays is now rounded to the nearest lower integer, i.e.,

$$N_{df} = \text{floor}\left(\frac{N - l - a}{F}\right) \tag{8}$$

Then, the compensating term is given by

$$\zeta = \text{round}\left(\left(\frac{N - l - a}{F}\right) - N_{df}\right). \tag{9}$$

Note that the total low-rate buffer also includes a term u_d to compensate for the preview required for the cubic splines upsampling, and is given by

$$N_s = N_d - u_d. \tag{10}$$

Since u_d is already at the low sampling rate, it does not need to be included in ζ.

4. Stability of multirate RC

In this section, stability conditions for multirate RC are developed. A sufficient condition for the stability of traditional RC systems for any buffer size N that is commonly used is given in the following Lemma [2]

Lemma 2. *The system* (2) *with repetitive controller R according to* (3) *is stable for all buffer lengths N if*

$$\sup_{\omega \in [0, \pi]} |Q(e^{i\omega})(1 - \alpha T(e^{i\omega})L(e^{i\omega}))| < 1. \tag{11}$$

Condition (11) applies to linear time-invariant (LTI) systems. The multirate repetitive control system, which includes down- and upsampling operations, is linear periodically time-varying (LPTV). The key idea to analyze the stability of multirate RC is to recast the LPTV system as an LTI system using a frequency-lifted reformulation. This is done in five steps. First, the system is separated into an LPTV and an LTI part. Second, the periodically time-varying nature of the multirate part is illustrated through an example of the impulse response. Third, frequency lifting is applied to both parts of the system. Fourth, a stability condition is provided in Theorem 4. Finally, Theorem 4 is extended by weighting in Theorem 5, which reduces the conservativeness of the stability conditions significantly.

Step 1: The LPTV part of the repetitive controller consists of the composition of the downsampling operator S_d, the low-rate buffer D_{N_s} for which $D_{N_s}(z) = z^{-N_s}$, the upsampling operator CS_u and the high-rate delay mismatch compensation D_ζ for which $D_\zeta(z) = z^{-\zeta}$, i.e., all terms in the forward path of the closed-loop multirate repetitive controller. This part of the system is denoted by $M = D_\zeta \circ CS_u \circ D_{N_s} \circ S_d$, and it maps a high-rate signal x to a delayed, approximated high-rate signal $\hat{x}_d$ as follows.

$$\hat{x}_d = M(x) = D_\zeta(CS_u(D_{N_s}(S_d(x)))). \tag{12}$$
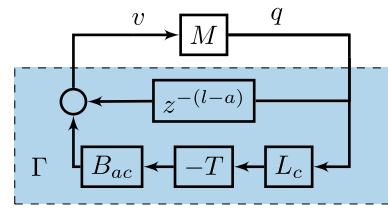

Fig. 9. Multirate scheme without external inputs.

The operator M is placed in feedback with the system consisting of the delay operator $z^{-(l-a)}$ in parallel with $G_a T L$, where T denotes the closed-loop system, as illustrated in Fig. 9. The system in the backward path is LTI and is given by

$$\Gamma = (z^{-(l-a)} - B_{ac} T L_c) = z^{-(l-a)}(1 - B_a T L). \tag{13}$$

Step 2: System M is a LPTV system with period F, for which the input–output behavior is described by the impulse response

$$\hat{x}_d(k) = \sum_{i=0}^{\infty} m_i(k) q^{-i} x(k) \tag{14}$$

$$= M(q, k) x(k), \tag{15}$$

with discrete time $k \in \{1, 2, \ldots, K\}$ for a total number of samples K and q denoting the forward shift operator for which $qv(k) = v(k + 1)$. The Markov parameters $m_i(k) \in \mathbb{R}$ are periodic with a period F, i.e., $m_i(k) = m_i(k + F)$. This is illustrated in the following example.

Example 3. Consider a system M consisting of the cubic splines upsampler CS_u in (7) for $F = 2$ with the corresponding downsampler S_d given in matrix form as

$$\begin{bmatrix} x_l(1) \\ x_l(2) \\ x_l(3) \\ x_l(4) \end{bmatrix} = \begin{bmatrix} 1 & 0 & 0 & 0 & 0 & 0 & 0 & 0 \\ 0 & 0 & 1 & 0 & 0 & 0 & 0 & 0 \\ 0 & 0 & 0 & 0 & 1 & 0 & 0 & 0 \\ 0 & 0 & 0 & 0 & 0 & 0 & 1 & 0 \end{bmatrix} \begin{bmatrix} x_h(1) \\ x_h(2) \\ \vdots \\ x_h(8) \end{bmatrix}.$$

The delay compensation is chosen as $\zeta = 0$ and the delay is chosen as $N_{df} = 2$ (corresponding to a four-sample delay in the high sampling rate), which is combined with the compensation $u_d = 2$ required for the preview in CS_u to give a total buffer size of $N_s = N_{df} - u_d = 0$. Then the impulse response of $M = CS_u \circ S_d$ for $K = 10$ samples is given by

$$\begin{bmatrix} \hat{x}_d(1) & \hat{x}_d(2) & \ldots & \hat{x}_d(10) \end{bmatrix}^\top =$$

$$\begin{bmatrix} 0 & 0 & 0 & 0 & 0 & 0 & 0 & 0 & 0 & 0 \\ -\frac{1}{16} & 0 & 0 & 0 & 0 & 0 & 0 & 0 & 0 & 0 \\ 0 & 0 & 0 & 0 & 0 & 0 & 0 & 0 & 0 & 0 \\ \frac{9}{16} & 0 & -\frac{1}{16} & 0 & 0 & 0 & 0 & 0 & 0 & 0 \\ 1 & 0 & 0 & 0 & 0 & 0 & 0 & 0 & 0 & 0 \\ \frac{9}{16} & 0 & \frac{9}{16} & 0 & -\frac{1}{16} & 0 & 0 & 0 & 0 & 0 \\ 0 & 0 & 1 & 0 & 0 & 0 & 0 & 0 & 0 & 0 \\ -\frac{1}{16} & 0 & \frac{9}{16} & 0 & \frac{9}{16} & 0 & -\frac{1}{16} & 0 & 0 & 0 \\ 0 & 0 & 0 & 0 & 1 & 0 & 0 & 0 & 0 & 0 \\ 0 & 0 & -\frac{1}{16} & 0 & \frac{9}{16} & 0 & \frac{9}{16} & 0 & -\frac{1}{16} & 0 \end{bmatrix} \begin{bmatrix} x(1) \\ x(2) \\ \vdots \\ x(10) \end{bmatrix},$$

with has Markov parameters that are periodic with a period of 2, i.e., $m_i(k) = m_i(k + 2)$. Also, $M(q, k) = M(q, k + 2)$ with, for example,

$$M(q, 7) = q^{-4},$$

$$M(q, 8) = -\frac{1}{16} q^{-1} + \frac{9}{16} q^{-3} + \frac{9}{16} q^{-5} - \frac{1}{16} q^{-7}.$$

Step 3: Next, system M is reformulated using frequency lifting. To explain the main idea of frequency lifting, consider the direct Fourier transform (DFT) $x(e^{j\omega})$ of the signal $x(k)$. The frequency-lifted

representation of $x(e^{j\omega})$ is denoted by $\mathbf{x}(e^{j\omega})$, and is of the form

$$\mathbf{x}(e^{j\omega}) = \begin{bmatrix} x^\mathsf{T}(e^{j\omega}) & x^\mathsf{T}(e^{j\omega}\phi) & \dots & x^\mathsf{T}(e^{j\omega}\phi^{F-1}) \end{bmatrix}^\mathsf{T}, \tag{16}$$

with $\phi = e^{j\frac{2\pi}{F}}$. Using the frequency-lifted signals $\mathbf{x}$ and $\hat{\mathbf{x}}_d$, the LPTV system M is transformed into a MIMO LTI system $\mathbf{M}(z)$ which has input–output behavior of the form

$$\hat{\mathbf{x}}_d = \mathbf{M}\mathbf{x}, \tag{17}$$

System $\mathbf{M}(z)$ is given by

$$\mathbf{M}(z) = G(z)\underline{M}(z^F)G^{-1}(z) \in \mathcal{R}^{F\times F}, \tag{18}$$

with $z = e^{j\omega}$ and

$$G(z) = \begin{bmatrix} I & z^{-1}I & \dots & z^{-F+1}I \\ I & (z\phi)^{-1} & \dots & (z\phi)^{-F+1} \\ \vdots & \vdots & & \vdots \\ I & (z\phi^{F-1})^{-1} & \dots & (z\phi^{F-1})^{-F+1} \end{bmatrix}. \tag{19}$$

The entries of $\underline{M}(e^{j\omega})$ are given by

$$\underline{M}_{[p,k]}(e^{j\omega}) = \tag{20}$$

$$\frac{e^{j\omega(p-k)\frac{1}{F}}}{F} \sum_{f=0}^{F-1} M\left(e^{j\omega\frac{1}{F}}\phi^{f\frac{1}{F}}, p-1\right)\phi^{f(p-k)\frac{1}{F}},$$

where $p, k \in \{1, 2, \dots, F\}$. For these notations and frequency-lifting in general, see, e.g., [17, Chapter 6]. The operator Γ is LTI, but for analysis purposes time lifting is applied similar as for M, leading to the diagonal, MIMO LTI system Γ.

Step 4: Reformulating the LPTV system M and the LTI system Γ through frequency lifting leads to two MIMO LTI systems $\mathbf{M}$ and Γ, through which stability of the multirate repetitive control system can be analyzed. Since frequency lifting is a norm-preserving operation [18], it holds that

$$\|M(q,\cdot)\|_\infty = \|\mathbf{M}(z)\|_\infty = \sup_{\omega\in[0,2\pi]} \bar{\sigma}(\mathbf{M}(e^{j\omega})). \tag{21}$$

This property is exploited in the following theorem.

Theorem 4. *Given a closed-loop system* (1) *with a stable complementary sensitivity T, and a stable learning filter L. Then the closed-loop system with multirate repetitive controller in* Fig. 8 *is stable if*

$$\sup_{\omega\in[0,2\pi]} \bar{\sigma}(\Gamma(e^{j\omega})\mathbf{M}(e^{j\omega})) < 1, \tag{22}$$

with $\mathbf{M}$ and Γ the frequency-lifted representations of M and Γ.

The proof of Theorem 4 is given in the Appendix.

Step 5: Because lifting the LTI system Γ leads to a diagonal MIMO LTI system Γ, the small-gain theorem employed in Theorem 4 can be made less conservative through scaling with an invertible diagonal matrix W. This leads to the following theorem.

Theorem 5. *Given a closed-loop system* (1) *with a stable complementary sensitivity T, and a stable learning filter L. Then the closed-loop system with multirate repetitive controller in* Fig. 8 *is stable if*

$$\|\Gamma W\mathbf{M}W^{-1}\|_\infty < 1, \tag{23}$$

for some invertible diagonal matrix W, and with $\mathbf{M}$ and Γ the frequency-lifted representations of M and Γ.

The proof of Theorem 5 is given in the Appendix. The matrix W can be a transfer function matrix, i.e., the scaling may be frequency-dependent. This is a well-known approach in the field of robust control, see, e.g., [19, Chapter 11]. Using that

$$\|\Gamma\mathbf{M}\|_\infty = \sup_{\omega\in[0,2\pi]} \bar{\sigma}\left(\Gamma(e^{j\omega})\mathbf{M}(e^{j\omega})\right), \tag{24}$$
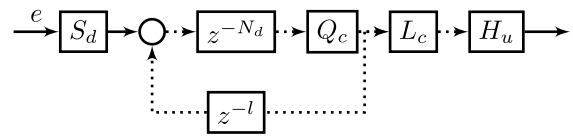

Fig. 10. Low-rate repetitive controller. All filters, including L and Q, are implemented at the low sampling rate, indicated by dotted lines. Down- and upsampling occur directly where the low-rate repetitive controller connects to the closed-loop system.

the condition in Theorem 4 can be visualized, which can be used to find a suitable scaling matrix W for a given Γ and $\mathbf{M}$. Alternatively, an optimization problem of the form

$$\sup_{\omega\in[0,2\pi]} \inf_{W_\omega\in\mathcal{W}} \bar{\sigma}\left(\Gamma(e^{j\omega})W_\omega(e^{j\omega})\mathbf{M}(e^{j\omega})W_\omega^{-1}(e^{j\omega})\right), \tag{25}$$

with $\mathcal{W}$ denoting the set of invertible diagonal transfer function matrices, can be solved pointwise in the frequency domain, as is commonly done in D-K iterations in μ-synthesis [19, Chapter 11.4].

5. Comparison to existing low-rate repetitive control

In the previous section, a new multirate repetitive controller is introduced, which in this section is compared to low-rate RC. Low-rate RC is an alternative existing approach in which the entire repetitive controller is placed at a reduced sampling rate, see, e.g., [5,9].

A low-rate repetitive controller is typically designed as shown in Fig. 10. Down- and upsampling occur directly where the low-rate repetitive controller connects to the high-rate closed-loop system, and all filters, including Q and L, are implemented at the low sampling rate f_l. In this case the low-rate buffer length is given by

$$N_d = \text{round}\left(\frac{N}{F}\right) - l - q, \tag{26}$$

where the compensating delays l and q are already in the low-rate. The low-rate repetitive control structure has three disadvantages compared to the multirate RC introduced in this paper.

- The low-rate structure as illustrated in Fig. 10 does not include an anti-aliasing filter before the downsampling, or an anti-imaging filter after the upsampling.
- Designing the L filter at a low sampling rate typically leads to a less accurate approximation of T^{-1} around the low-rate Nyquist frequency. Since the aim of low- and multirate RC is to attenuate disturbances up to $\frac{f_l}{2}$, this leads to reduced performance. Due to the noble identity, $L(z)H_{u,F} \equiv H_{u,F}L(z^F)$, with $H_{u,F}$ an upsampler with an upsampling factor F [20, Chapter 4.2]. This illustrates that designing and implementing L at a low sampling rate before the upsampler reduces the design freedom compared to designing L directly at the high rate.
- Most importantly, because the complete controller is implemented at f_l, it is not possible to include compensation for the period discrepancies between the original buffer N and the low-rate buffer N_l.

While the first disadvantage is easy to remedy by including these filters before downsampling and after upsampling, the second and third disadvantage can become problematic. If $\frac{N}{F}$ is not close to an integer, the discrepancy between the period of the disturbance and that of the low-rate RC becomes large, which leads to a significantly reduced performance. In Section 6, the performance of multirate RC is compared to that of the low-rate RC illustrated in Fig. 10.

6. Experimental results

In this section, the proposed multirate repetitive controller is applied in a case study using the industrial print-belt system introduced

in Section 2 and compared to two related methods: traditional and low-rate RC. First, the design procedure for multirate RC is summarized. Second, the repetitive controllers are introduced and third, experimental results are presented.

6.1. Design procedure for multirate RC

The design procedure for multirate repetitive control is largely similar to that for standard RC. The procedure is summarized in Procedure 6, which is further illustrated in the case study in the next subsection.

Procedure 6 Multirate RC design

1: Determine the frequency of the disturbance to be attenuated, and the number of relevant higher harmonics, to determine N and F.
2: Design learning filter L to approximate T^{-1}, for example using ZPETC [16].
3: Design the anti-aliasing filter B_a based on the Nyquist frequency of the low sampling rate.
4: Compute $\mathbf{M}(z)$ and $\mathbf{\Gamma}(z)$ according to Section 4 and check Condition (22) in Theorem 4.
5: If Condition (22) is not met due to model mismatch at high frequencies, include a robustness filter Q, for example based on Condition (11) for standard RC with $\alpha = 1$.
6: If Condition (22) is still not met, try to find W such that Condition (23) in Theorem 5 is met. If no such W can be found, redesign Q or B_a.
7: Given the filters and their causal counterparts, compute ζ according to (9).
8: Select α based on system safety requirements and the prevalence of disturbances that are not periodic with N.

6.2. Multirate, low-rate and traditional repetitive control configurations

The multirate repetitive controller is applied to the industrial print-belt system shown in Fig. 1. As illustrated in Section 2, the system contains different types of periodic disturbances at varying frequencies. The focus is on two particular disturbances, caused by the low-speed and high-speed drive belts. These disturbances occur at respectively 1.7 Hz and 5.4 Hz, as shown in Fig. 3, and they have a small number of approximately 15 and 7 relevant higher harmonics that are visible up to 50 Hz. Three different repetitive controllers are employed to attenuate the disturbances caused by the drive belts. Because disturbances have relevant higher harmonics up to 50 Hz, the low-rate sampling frequency for the low- and multirate repetive controllers is chosen as $f_l = 100$ Hz. The original high-rate sampling frequency of the system is $f_h = 500$ Hz, resulting in a sampling ratio of $F = 5$.

The identified frequency response and a model of the closed loop T are shown in Fig. 11. The transfer function of the estimated model is given by

$$\hat{T}(z) = \tag{27}$$
$$\frac{0.0007698z - 0.0006865}{z^5 - 4.513z^4 + 8.386z^3 - 8.041z^2 + 3.979z - 0.8111}.$$

Using ZPETC [16], a high-rate learning filter $L \approx \hat{T}^{-1}$ is designed. For the low-rate RC this filter is downsampled to 100 Hz. To enable a fair comparison, low-rate RC is implemented with the anti-aliasing filter and the cubic splines upsampler that are also used for multirate RC. The anti-aliasing filter B_a is a fourth-order Butterworth lowpass filter with a cutoff frequency of 42.5 Hz. In addition, a 20th-order FIR lowpass anti-imaging filter with a cutoff frequency of 20 Hz is included in the multirate RC, which is identical to the Q-filter in the traditional RC configuration. The Q-filter for the low-rate RC is a second-order FIR lowpass filter. All implementations use a learning gain $\alpha < 0.3$ to ensure safe operation. The stability is ensured using a weighting filter W according to Theorem 5.
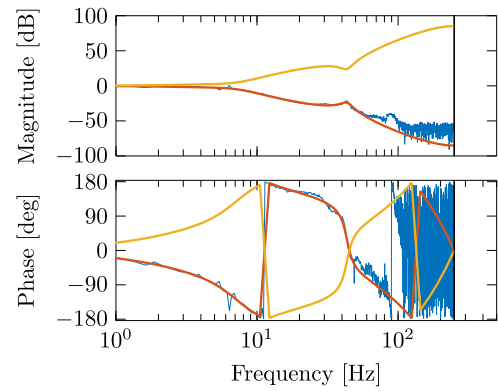

Fig. 11. Bode diagrams of the measured frequency response of T (——), the model $\hat{T}$ (——) and the learning filter $L \approx \hat{T}^{-1}$ (——).

Table 1
Number of delays used in the traditional repetitive controller (RC), multirate repetitive controller (MRC) and low-rate repetitive controller (LRC) for the low-speed drive belt (LSDB) and high-speed drive belt (HSDB).

Delay	RC	MRC	LRC
N LSDB	290	58	58
N HSDB	92	18	18
q	10	10	–
q_s	–	2	1
l	4	4	–
l_s	–	1	4
a	–	10	10
a_s	–	2	2
Total N_s LSDB	276	51	53
Total N_s HSDB	78	13	11
ζ LSDB	–	1	–
ζ HSDB	–	3	–

The number of delays used in the different repetitive controllers are listed in Table 1. Note that the filters used to compensate the disturbances caused by either the low-speed or the high-speed drive belt are identical, but the buffer length differs depending on the disturbance frequency. In particular, the disturbance originating from the low-speed drive belt occurs at 1.724 Hz, leading to buffer lengths of $N = 290$ at 500 Hz and $N = 58$ at 100 Hz. The disturbance originating from the high-speed drive belt occurs at 5.421 Hz, leading to buffer lengths of $N = 92$ at 500 Hz and $N = 18$ at 100 Hz.

6.3. Experimental results

The performance of the different repetitive control configurations is compared when compensating the disturbances caused by either the low-speed drive belt, the high-speed drive belt, or both. For each case the cumulative power-spectral densities (CPSD) of the error are compared. For the compensation of the low-speed drive belt, the performance of multirate RC matches that of traditional repetitive control, yet with significantly lower memory usage. The corresponding CPSD in Fig. 12 illustrates that all three methods compensate the disturbance around 1.7 Hz well. However, low-rate repetitive control leads to more error content at high frequencies, which may be caused by differences in the Q-filter due to the low-rate implementation.

Next, the different RC approaches are used to compensate the disturbance caused by the high-speed drive belt, which has a base frequency of approximately 5.4 Hz. Multirate RC performs similar to traditional RC, whereas low-rate RC is not able to attenuate this disturbance well, as is also illustrated in the CPSD in Fig. 13. In this figure, the error peak at 5.4 Hz is eliminated by traditional and multirate RC, yet low-rate RC is not able to compensate this disturbance due to a significant mismatch
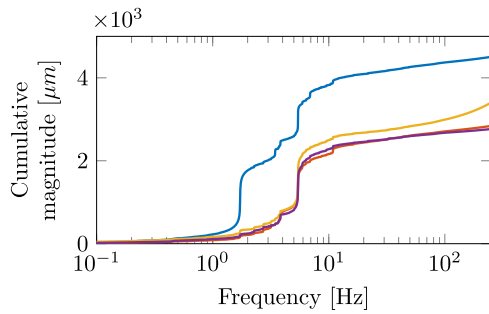
Fig. 12. Cumulative error spectrum without compensation (——) and with compensation of the disturbance originating from the low-speed drive belt. Multirate RC (——) matches the performance of traditional RC (——), while the error for low-rate RC (——) is higher, especially at high frequencies.
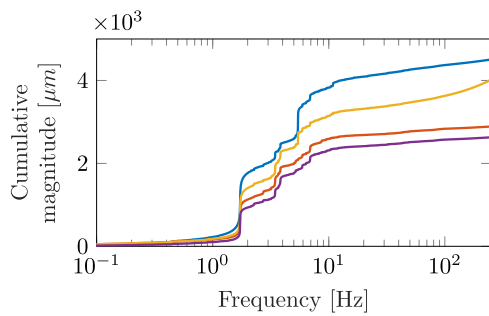

Fig. 13. Cumulative error spectrum without compensation (——) and with compensation of the disturbance originating from the high-speed drive belt. Multirate RC (——) leads to a slightly reduced performance compared to traditional RC (——), but both approaches compensate the disturbance at 5.4 Hz completely. Low-rate RC (——) is not able to compensate this disturbance well due to the period mismatch, leading to a much higher error.

Fig. 14. Error over time without compensation (——) and with compensation of the disturbance originating from both drive belts. Multirate RC (——) and traditional RC (——) achieve similar small errors, and outperform low-rate RC (——), the error of which still contains the 5.4 Hz component caused by the high-speed drive belt.

Fig. 15. Cumulative error spectrum without compensation (——) and with compensation of the disturbances originating from both drive belts. Multirate RC (——) is able to match the performance of traditional RC (——), while low-rate RC (——) cannot attenuate the disturbance at 5.4 Hz due to the period mismatch.

in frequencies. The buffer length of 92 samples at 500 Hz cannot be approximated well at 100 Hz, see also Example 1. In multirate RC, this is compensated by the additional delay of ζ samples at the high sampling rate, leading to a similar performance as traditional RC, while reducing the memory usage.

Lastly, the RC approaches are applied to the disturbances caused by the low-speed and high-speed drive belts simultaneously. Convergence criteria for this case, which uses two separate RC controllers in parallel, can be developed using sequential design techniques along the lines of [21], yet this is outside the scope of this paper. The experimental results demonstrate that also for this case, multirate RC is able to match the performance of traditional RC while reducing the memory usage significantly. Both approaches lead to low errors, as shown in Fig. 14 which shows the error in the time domain. The corresponding CPSD in Fig. 15 shows that both disturbances are compensated almost completely by multirate RC and traditional RC. In contrast, low-rate RC is not able to compensate the disturbance at 5.4 Hz due to the period length mismatch.

Remark 7. The presented results show a significant reduction in tracking error compared to low-rate RC. This enables, for example, increased print belt velocities in industrial printing systems. In addition, compared to standard RC, the buffer size is reduced by a factor five in this example while the performance is retained. While the buffer size may not be a limiting factor for a single repetitive controller, this is relevant for systems with many periodic disturbances that each require a dedicated RC buffer.
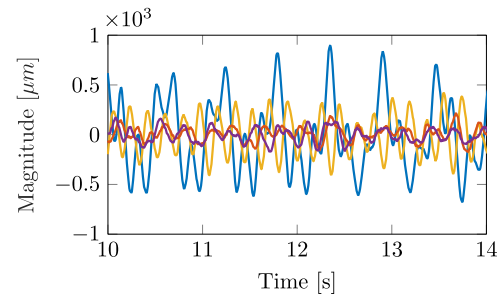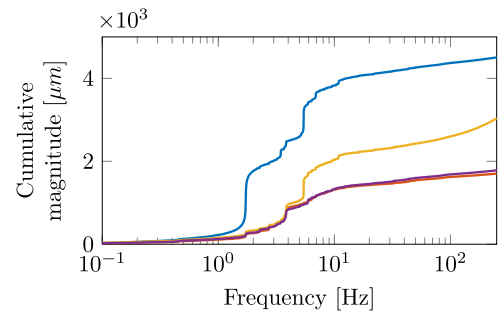
7. Conclusion

A new multirate repetitive controller is introduced that retains the performance of traditional repetitive control while significantly reducing the memory usage. This is accomplished by implementing only the buffer of the repetitive controller at a reduced sampling rate, while the learning filter is implemented at the original sampling rate. This configuration enables the introduction of an additional filter that compensates the period mismatch between the low-rate buffer and the high-rate periodic disturbance. Stability criteria for the resulting linear periodic time-varying system are developed. Experimental implementation on an industrial print-belt system demonstrates that multirate RC achieves the same performance as a traditional RC, outperforming a low-rate repetitive controller that implements all filters at a reduced sampling rate. Future research should consider convergence criteria for the case with multiple multirate repetitive controllers in parallel, as well as other combinations of regular and multirate repetitive controllers, possibly along the lines of the sequential design techniques in [21].

CRediT authorship contribution statement

Leontine Aarnoudse: Conceptualization, Formal analysis, Writing – original draft, Writing – review & editing. **Kevin Cox:** Conceptualization, Software, Writing – review & editing. **Sjirk Koekebakker:** Conceptualization, Software, Supervision, Writing – review & editing. **Tom Oomen:** Conceptualization, Funding acquisition, Supervision, Writing – review & editing.

Declaration of competing interest

The authors declare that they have no known competing financial interests or personal relationships that could have appeared to influence the work reported in this paper.
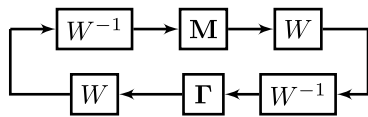
Fig. 16. Inclusion of weighting filter W in the loop. Since $\boldsymbol{\Gamma}$ is diagonal, $W\boldsymbol{\Gamma}W^{-1} = \boldsymbol{\Gamma}$ and therefore $\boldsymbol{\Gamma}WMW^{-1} = \boldsymbol{\Gamma}\mathbf{M}$.

Data availability

No data was used for the research described in the article.

Appendix

In this appendix the proofs of Theorems 4 and 5 are provided.

Proof of Theorem 4. Since lifting is a norm-preserving operation, it holds that

$$\sup_{\omega\in[0,2\pi)} \bar{\sigma}(\boldsymbol{\Gamma}(e^{j\omega})\mathbf{M}(e^{j\omega})) = \|\Gamma(q)M(q,\cdot)\|_\infty. \tag{28}$$

By the small-gain theorem, a sufficient condition for the input–output stability of a system G is that the loop gain $\|G\|_\infty < 1$. It follows that

$$\sup_{\omega\in[0,2\pi)} \bar{\sigma}(\boldsymbol{\Gamma}(e^{j\omega})\mathbf{M}(e^{j\omega})) < 1, \tag{29}$$

is a sufficient condition for the stability of the multirate repetitive control system. □

Proof of Theorem 5. Consider the insertion of $WW^{-1} = I$ before and after M in the loop as illustrated in Fig. 16. Since $\boldsymbol{\Gamma}$ is diagonal, $W\boldsymbol{\Gamma}W^{-1} = \boldsymbol{\Gamma}$. It follows that

$$\boldsymbol{\Gamma}WMW^{-1} = \boldsymbol{\Gamma}\mathbf{M}, \tag{30}$$

and therefore, by Theorem 4,

$$\|\boldsymbol{\Gamma}WMW^{-1}\|_\infty < 1, \tag{31}$$

is a sufficient condition for the stability of the closed-loop system with a multirate repetitive controller. □

References

[1] Tomizuka M, Tsao T-C, Chew K-K. Analysis and synthesis of discrete-time repetitive controllers. J Dyn Syst Meas Control 1989;111:353–8. http://dx.doi.org/10.1115/1.3153060.

[2] Longman RW. On the theory and design of linear repetitive control systems. Eur J Control 2010;16(5):447–96. http://dx.doi.org/10.3166/ejc.16.447-496.

[3] Francis B, Wonham W. The internal model principle of linear control theory. Automatica 1976;12:457–65. http://dx.doi.org/10.1016/s1474-6670(17)67756-5.

[4] Hillerström G, Sternby J. Repetitive control using low order models. In: Am. control conf.. Baltimore, Maryland, USA; 1994, p. 1873–8. http://dx.doi.org/10.1109/ACC.1994.752398.

[5] Sadegh N, Hu AP, James C. Synthesis, stability analysis, and experimental implementation of a multirate repetitive learning controller. J Dyn Syst Meas Control Trans ASME 2002;124(4):668–74. http://dx.doi.org/10.1115/1.1514060.

[6] Kempf C, Tomizuka M, Horowitz R, Messner W. Comparison of four discrete-time repetitive control algorithms. IEEE Control Syst 1993;13(6):48–54. http://dx.doi.org/10.1109/37.248004.

[7] Cuiyan L, Dongchun Z, Xianyi Z. A survey of repetitive control. In: 2004 IEEE/RSJ int. conf. intell. robot. syst.. vol. 2, 2004, p. 1160–6. http://dx.doi.org/10.1109/iros.2004.1389553.

[8] Shi Y, Longman RW, Nagashima M. Small gain stability theory for matched basis function repetitive control. Acta Astronaut 2014;95(1):260–71. http://dx.doi.org/10.1016/j.actaastro.2013.09.016.

[9] Zhang B, Zhou K, Wang D. Multirate repetitive control for PWM DC/AC converters. IEEE Trans Ind Electron 2014;61(6):2883–90. http://dx.doi.org/10.1109/TIE.2013.2274423.

[10] Fujimoto H, Kawakami F, Kondo S. Multirate repetitive control and applications. In: Am. control conf.. 2004, p. 2875–80. http://dx.doi.org/10.1109/acc.2003.1243759.

[11] Fujimoto H. RRO compensation of hard disk drives with multirate repetitive perfect tracking control. IEEE Trans Ind Electron 2009;56(10):3825–31. http://dx.doi.org/10.1109/TIE.2009.2017558.

[12] Nagahara M, Yamamoto Y. Digital repetitive controller design via sampled-data delayed signal reconstruction. Automatica 2016;65:203–9. http://dx.doi.org/10.1016/j.automatica.2015.11.0290.

[13] Wang D, Chen X. A Multirate Repetitive Control for Fractional-order Servos in Laser-based Additive Manufacturing. In: Am. control conf.. AACC; 2018, p. 4831–6. http://dx.doi.org/10.23919/ACC.2018.8431385.

[14] Xie C, Zhao X, Savaghebi M, Meng L, Guerrero JM, Vasquez JC. Multirate fractional-order repetitive control of shunt active power filter suitable for microgrid applications. IEEE J Emerg Sel Top Power Electron 2017;5(2):809–19. http://dx.doi.org/10.1109/JESTPE.2016.2639552.

[15] Chang WS, Suh IH, Kim TW. Analysis and design of two types of digital repetitive control systems. Automatica 1995;31(5):741–6. http://dx.doi.org/10.1016/0005-1098(94)00156-D.

[16] Tomizuka M. Zero phase error tracking algorithm for digital control. J Dyn Syst Meas Control 1987;109:65–8. http://dx.doi.org/10.1115/1.3143866.

[17] Bittanti S, Colaneri P. Periodic Systems: Filtering and Control. London: Springer-Verlag London Limited; 2009, http://dx.doi.org/10.1007/978-1-84800-911-0.

[18] Zhang C, Zhang J, Furuta K. Analysis of H2 and H-infinity performance of discrete periodically time-varying controllers. Automatica 1997;33(4):619–34. http://dx.doi.org/10.1016/S0005-1098(96)00224-5.

[19] Zhou K, Doyle JC, Glover K. Robust and optimal control. Englewood Cliffs, New Jersey: Prentice Hall; 1996.

[20] Vaidyanathan P. Multirate systems and filter banks. Prentice Hall; 1993.

[21] Blanken L, Koekebakker S, Oomen T. Multivariable Repetitive Control: Decentralized Designs with Application to Continuous Media Flow Printing. IEEE/ASME Trans Mechatronics 2020;25(1):294–304. http://dx.doi.org/10.1109/TMECH.2019.2951609.

Leontine Aarnoudse received the B.Sc. degree (2017) and M.Sc. degree (cum laude) (2019) in Mechanical Engineering from the Eindhoven University of Technology, Eindhoven, The Netherlands. She is currently pursuing a Ph.D. degree in the Control Systems Technology group within the department of Mechanical Engineering at Eindhoven University of Technology. Her research interests are in the field of control for precision mechatronics, and are mostly centered around the development of learning theory for these systems.

Kevin Cox received the M.Sc. degree in Systems and Control with specialization in the Control Systems Technology group from the Eindhoven University of Technology, Eindhoven, The Netherlands, in 2023. His graduation project focused on repetitive control and was a collaboration between the TU/e and Canon Production Printing. He is currently a mechatronics engineer with ASML, Veldhoven, The Netherlands. His research interest is in the field of motion control and learning control techniques for applications in mechatronic systems.

S.H. Koekebakker received the M.Sc. and Ph.D. degrees in mechanical engineering from the Delft University of Technology, The Netherlands, in 1993 and 2001, respectively. Since 1999 he is working as a mechatronic designer within Canon Production Printing, formerly Océ Technologies B.V. As of 2009 he is also a parttime senior researcher in the Control Systems Technology group of the Mechanical Engineering Department of Eindhoven University of Technology. His main research interests are iterative learning and repetitive control, precision motion control and printing systems.

Tom Oomen is full professor with the Department of Mechanical Engineering at the Eindhoven University of Technology. He is also a part-time full professor with the Delft University of Technology. He received the M.Sc. degree (cum laude) and Ph.D. degree from the Eindhoven University of Technology, Eindhoven, The Netherlands. He held visiting positions at KTH, Stockholm, Sweden, and at The University of Newcastle, Australia. He is a recipient of the 7th Grand Nagamori Award, the Corus Young Talent Graduation Award, the IFAC 2019 TC 4.2 Mechatronics Young Research Award, the 2015 IEEE Transactions on

Control Systems Technology Outstanding Paper Award, the 2017 IFAC Mechatronics Best Paper Award, the 2019 IEEJ Journal of Industry Applications Best Paper Award, and recipient of a Veni and Vidi personal grant. He is currently a Senior Editor of IEEE Control Systems Letters (L-CSS) and Associate Editor of IFAC Mechatronics, and he has served on the editorial boards of the IEEE Control Systems Letters (L-CSS) and IEEE Transactions on Control Systems Technology. He has also been vice-chair for IFAC TC 4.2 and a member of the Eindhoven Young Academy of Engineering. His research interests are in the field of data-driven modeling, learning, and control, with applications in precision mechatronics.